11-2018

Characterization and Effect of Metal Ions on the Formation of the *Thermus thermophilus* Sco Mixed Disulfide Intermediate

Liezelle C. Lopez
Trinity University, llopez@trinity.edu

Nikita Mukhitov
Trinity University, nmukhito@trinity.edu

Lindsey D. Handley
Trinity University, lhandley@trinity.edu

Cristina S. Hamme
Trinity University, chamme@trinity.edu

Cristina R. Hofman
Trinity University, chofman@trinity.edu

See next page for additional authors

THE PROTEIN SOCIETY

Characterization and effect of metal ions on the formation of the *Thermus thermophilus* Sco mixed disulfide intermediate

Liezelle C. Lopez,[1,2] Nikita Mukhitov,[1,3] Lindsey D. Handley,[1,4] Cristina S. Hamme,[1,5] Cristina R. Hofman,[1] Lindsay Euers,[1,6] Jennifer R. McKinney,[1,7] Amani D. Piers,[1,8] Ellen Wadler,[1,9] and Laura M. Hunsicker-Wang[1]*

[1]Department of Chemistry, Trinity University, One Trinity Place, San Antonio, Texas, 78212-7200
[2]Baylor School of Medicine, One Baylor Plaza, Houston, Texas, 77030
[3]Department of Biological Engineering, Massachusetts Institute of Technology, Cambridge, Massachusetts, 02139
[4]ThoughtSTEM, San Diego, California, 92108
[5]Lone Star Family Health Center, Conroe, Texas, 77034
[6]Houston Methodist Hospital, Houston, Texas, 77303
[7]Department of Maternal Fetal Medicine, Baylor College of Medicine, One Baylor Plaza, Houston, Texas, 77004
[8]Department of Psychology, Drexel University, Philadelphia, Pennsylvania, 19104
[9]University of Texas Health Science Center Houston School of Public Health, Houston, Texas, 77030

Received 30 June 2018; Accepted 23 August 2018
DOI: 10.1002/pro.3502
Published online 3 October 2018 proteinscience.org

Abstract: The Sco protein from *Thermus thermophilus* has previously been shown to perform a disulfide bond reduction in the Cu_A protein from *T. thermophilus*, which is a soluble protein engineered from subunit II of cytochrome ba_3 oxidase that lacks the transmembrane helix. The native cysteines on *Tt*Sco and *Tt*Cu_A were mutated to serine residues to probe the reactivities of the individual cysteines. Conjugation of TNB to the remaining cysteine in *Tt*Cu_A and subsequent release upon incubation with the complementary *Tt*Sco protein demonstrated the formation of the mixed disulfide intermediate. The cysteine of *Tt*Sco that attacks the disulfide bond in the target *Tt*Cu_A protein was determined to be *Tt*Sco Cysteine 49. This cysteine is likely more reactive than Cysteine 53 due to a higher degree of solvent exposure. Removal of the metal binding histidine, His 139, does not change MDI formation. However, altering the arginine adjacent to the reactive cysteine in Sco (Arginine 48) does alter the formation of the MDI. Binding of Cu^{2+} or Cu^{+} to *Tt*Sco prior to reaction with *Tt*Cu_A was found to preclude formation of the mixed disulfide intermediate. These results shed light on a mechanism of disulfide bond reduction by the *Tt*Sco protein and may point to a possible role of metal binding in regulating the activity.

Importance: The function of Sco is at the center of many studies. The disulfide bond reduction in Cu_A by Sco is investigated herein and the effect of metal ions on the ability to reduce and form a mixed disulfide intermediate are also probed.

Keywords: Sco; Cu_A; TNB; thiol-disulfide oxidoreductase; mixed disulfide intermediate; disulfide bonds; copper metal binding; metalloproteins

Additional Supporting Information may be found in the online version of this article.

Grant sponsor: National Science Foundation-Division of Chemistry; Grant number: CHE-1726441; Grant sponsor: National Science Foundation-Division of Undergraduate Education; Grant number: S-STEM 1153796; Grant sponsor: Research Corporation for Science Advancement; Grant number: 7693; Grant sponsor: Welch Foundation; Grant number: W-0031.

*Correspondence to: Laura Hunsicker-Wang, One Trinity Place San Antonio, TX 78212, USA. E-mail: lhunsick@trinity.edu

Introduction

The Sco protein family has been shown to be involved in the assembly of cytochrome *c* oxidase; however, the exact role that Sco plays has been the subject of much study and debate.[1–13] The family of Sco proteins encompasses Sco1 and Sco2, which are found in humans and yeast, as well as related proteins in many other bacteria.[14–19] Early studies suggested a role as a possible copper chaperone in the assembly of the Cu_A site of cytochrome *c* oxidase[14,15,20,21] Additional research has also suggested roles in redox signaling and/or copper homeostasis as well as implications that Sco can be involved in the assembly of the Cu_B site.[8,10,22,23]

The thiol/disulfide oxidoreductase role for Sco was proposed in part as the result of structural characterizations that revealed similarities to thioredoxins and peroxiredoxins including the βαβαββα-fold characteristic of thioredoxins.[3,8,10,22,24,25] These similarities in motifs make it plausible that Sco can play a redox role. One suggested role for Sco is the ability to reduce the disulfide bond present in the Cu_A site prior to copper insertion (Fig. 1). The Sco protein from *Thermus thermophilus* (*Tt*Sco) (Fig. S1) has been shown to be capable of reducing the disulfide bond in the *T. thermophilus* Cu_A (*Tt*Cu_A), and a separate protein, *Tt*PCu_AC, delivers copper to the site to form the binuclear center.[3]

The search for a deep understanding of the function of Sco is complicated by the protein's additional potential to bind metals. A conserved CXXXC motif along with a conserved histidine farther away in primary sequence is found in all Sco proteins.[22] The conserved cysteines and histidine are all thought to be involved in binding metals, including Cu^{1+} or Cu^{2+} *in vivo*, and have been shown to bind a variety of different metal ions *in vitro*.[1,6,26–29] There remains unknown aspects of Sco reactivity, and it is not even clear if the role(s) of Sco in different species is the same,[12,13] however, the known specific and distinct roles of Sco in prokaryotes and mammals include disulfide bond reduction.[3,7,30]

In the study presented here, the thiol/disulfide oxidoreductase role is closely investigated for *Tt*Sco. The mechanism of the disulfide bond reduction is probed and subsequently the cysteine residues on *Tt*Sco and *Tt*Cu_A that are involved in the formation of the mixed disulfide intermediate (MDI) are elucidated. The effects of metal binding on the formation of the MDI, and how different mutagenesis of important resides affect MDI formation are also explored.

Results

Finding the reactive cysteines forming the MDI

Thioredoxins have been shown to be able reduce disulfide bonds through a two-step, bimolecular, nucleophilic attack mechanism involving a mixed-disulfide intermediate.[31] In the first step, the thioredoxin's most reactive cysteine thiol attacks the sulfur of the disulfide bond of its target, forming a mixed-disulfide intermediate. Subsequently, the adjacent thiol on the thioredoxin attacks the mixed disulfide bond, resulting in a reduced target and an oxidized thioredoxin. Due to the similarity in fold and the reactive cysteine motif, it is possible that *Tt*Sco can follow a similar mechanism, passing through the postulated mixed disulfide intermediate (MDI) [Fig. 2(A)].

In order to probe this mechanism for Sco proteins, single cysteine-to-serine mutations were made in both *Tt*Sco and *Tt*Cu_A. These mutations allow formation of MDI, but force the reaction to stop after the first step of the overall thioredoxin mechanism due to the lack of adjacent thiols that would complete the mechanism [Fig. 2(B)]. This setup yielded four possible cysteine pairs as candidates for the most reactive biological pair. In turn, comparison of the reactivities of all the pairs also elucidated the residues involved in the first step of the *Tt*Cu_A disulfide reduction pathway.

In *Tt*Sco, the only two cysteine residues are the two conserved cysteines of the CXXXC motif, *Tt*Sco cysteine 49 and *Tt*Sco cysteine 53.[1] In *Tt*Cu_A, the only two cysteines are *Tt*Cu_A cysteine 149 and *Tt*Cu_A cysteine 153, which are the cysteines bound to copper in the assembled, holoprotein. Following removal of a single cysteine by mutagenesis, the remaining cysteine in the mutant *Tt*Cu_A was labeled using 5,5′-dithiobis-(2-nitrobenzoic acid) (DTNB), which covalently attaches a chromophore (2-nitro-5-thiobenzoate, TNB). This setup allowed for probing which cysteine is more reactive in *Tt*Sco and which cysteine is attacked in *Tt*Cu_A. Using TNB-labeled *Tt*Cu_A, the attack on mutant *Tt*Cu_A by mutant *Tt*Sco resulted in release of the conjugated TNB moiety [Fig. 2(A)]. Thus, this method conveniently converted the reaction to a format that can be easily monitored as a function of released chromophore (TNB) using UV–visible spectroscopy. Furthermore, the liberation of the chromophore is then logically interpreted as the formation of the MDI. Since the TNB can be conjugated to only one possible cysteine, this assay is ideal for a reactivity comparison and has been used to probe thioredoxins previously.[31]

Joint incubation of each possible combination of proteins at a 1:1 ratio resulted in the liberation of the TNB chromophore which was monitored as an increase in absorbance at 412 nm (Fig. S2). It was noted that the amount of TNB conjugated to the cysteine in the *Tt*Cu_A proteins differ between the different mutants and protein labeling preparations. The reactions are therefore plotted as a percentage of the

[1]The naming of the cysteine residues will be: name of protein cysteine number. This convention is used for clarity since the numbering of the pertinent cysteines in both proteins are similar.

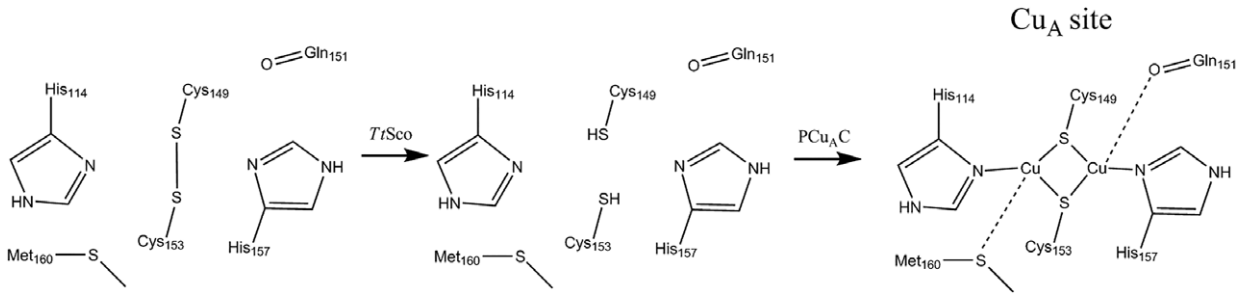

Figure 1. Proposed assembly of the Cu_A site. *Tt*Sco reduces a disulfide bond in apo-*Tt*Cu_A and then PCu_AC transfers copper ions to fully metallate the site.

TNB released in order to normalize for the amount of TNB that is conjugated to the *Tt*Cu_A protein initially [Fig. 3(A)]. Each pair is named indicating which cysteine is retained (e.g. Sco-Cys49: CuA-Cys153 is the reaction of the *Tt*Sco mutant C53S, in which cysteine 49 remains, and the *Tt*Cu_A mutant, C149S, in which cysteine 153 remains).

Accounting for the amount of TNB initially conjugated to Cu_A effectively normalized for the difference in solvent accessibility of Cysteines 149 and 153. Furthermore, this normalization addresses a potential bias produced by solvent accessibility. When comparing the data as the absorbance (412 nm) over time (Fig. S2) with the % TNB release over time, a change in the order of reactivity is noted. Thus, the data will be analyzed using the %TNB conjugation.

In all of these experiments, one combination of mutants, Sco-Cys49:Cu_A-Cys153, clearly released more TNB and did so at a faster rate [Fig. 3(A)] than all of the other pairs. This finding brings to light the most reactive pair, suggesting that cysteine 49 on Sco attacks Cysteine 153 on Cu_A in the first step of the overall reduction mechanism. While this pair was the most reactive, the four other cysteine combinations do exhibit release of TNB. Thus, while one pair is most reactive, it is evident that all cysteines are capable of reaction to an extent.

SDS PAGE gels run in the absence of DTT or other reducing agent allowed for the detection and the evaluation of the MDI and protein dimers. The MW of the MDI, the species composed of the linked *Tt*Sco and *Tt*Cu_A proteins, is ≈ 33 kDa, the *Tt*Sco dimer is ≈ 38 kDa, and the *Tt*Cu_A dimer is ≈ 28 kDa. After incubation, the mixed disulfide intermediate is observed at the correct molecular weight [Fig. 3(B)] and is in the highest concentration for the Sco-Cys49:Cu_A-Cys153 pair, consistent with TNB release data.

The different evaluative methods (%TNB released and A_{412} nm) are both driven by the same residue for the two most reactive pairs. When evaluating the % TNB released, Sco-Cys49 is present in the most reactive pairs [Fig. 3(A)] whereas in the

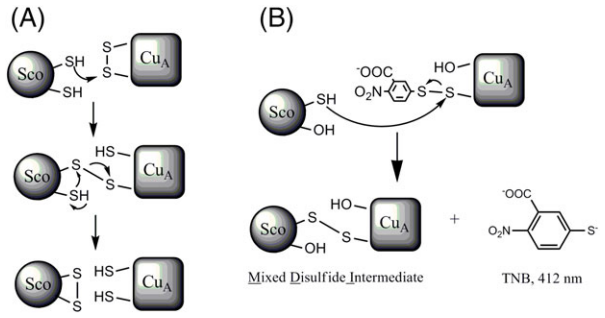

Figure 2. (A) Proposed mechanism of disulfide bond reduction based on the thioredoxin mechanism. (B) Trapping of the mixed disulfide intermediate using cysteine-to-serine mutants and release of the TNB chromophore. (A) and (B) are based on similar work with thioredoxins.[31]

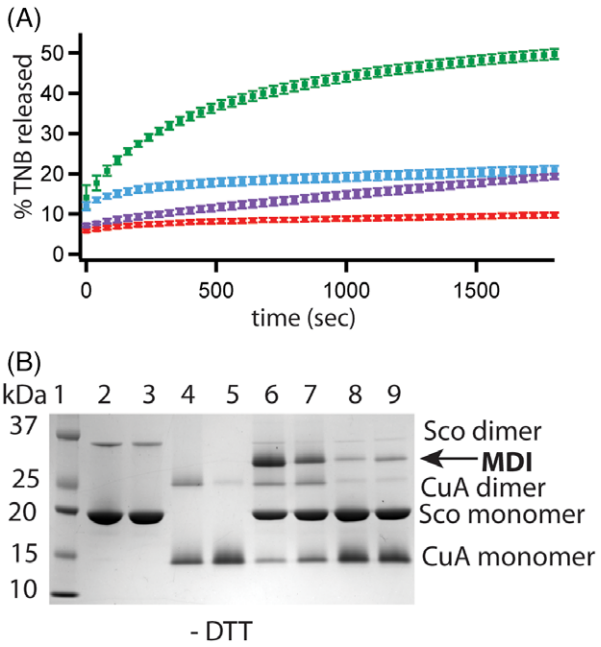

Figure 3. MDI formation. (A) Percent of TNB released from *Tt*Cu_A after incubation of pairs of mutant proteins ([TNB released]/ [TNB possible to release]). Green: *Tt*Sco-Cys49:*Tt*Cu_A-Cys153, Blue: *Tt*Sco-Cys49:*Tt*Cu_A-Cys149 Grey: *Tt*Sco-Cys53:*Tt*Cu_A-Cys153, Red: *Tt*Sco-Cys53:*Tt*Cu_A-Cys149, B) SDS-PAGE gel run in the absence of DTT of representative reactions. Lane 1 MW ladder, Lane 2 *Tt*Sco-Cys53, Lane 3 *Tt*Sco-Cys49, Lane 4 *Tt*Cu_A-Cys149, Lane 5 *Tt*Cu_A-Cys153, Lane 6 *Tt*Sco-Cys49:*Tt*Cu_A-Cys153, Lane 7 *Tt*Sco-Cys53:*Tt*Cu_ACys153, Lane 8 *Tt*Sco-Cys49:*Tt*Cu_A-Cys149, Lane 9 *Tt*Sco-Cys53:*Tt*Cu_A-Cys 149.

non-normalized graph (Fig. S2), Cu_A-Cys153 is the common cysteine residue in the most reactive pairs. Thus, the two different characterization methods bring to light different aspects of the reaction mechanism that work together in the function of *Tt*Sco. This comparison suggests that when normalized for accessibility, Sco-Cys49 is clearly more *nucleophilic* than Cys53; on the other hand, Cu_A-Cys153 is the most accessible, supported with determined larger degrees of TNB conjugation (see below).

The amount of TNB released allows for inferring the reactivity and accessibility of the cysteine residue of interest. Exposing reduced protein to DTNB will result in TNB conjugation to only the single cysteine in each of the proteins. The more nucleophilic and/or more accessible cysteine residue will in turn attack DTNB with a higher frequency, thus leading to more covalent attachment of TNB to the protein. Release of the tag from the protein by DTT will then quantify the total amount of covalently bound TNB (% conjugated) and thus elucidate the cysteine reactivity and accessibility. For the Sco mutants, Sco-Cys49 released more TNB than Sco-Cys53. Likewise, Cu_A-Cys153 released more than Cu_A-Cys149 (Table I). Interestingly, if the TNB is conjugated to Cu_A-Cys153 and reacted with reduced Sco, MDI formation is also observed, but with a lower amount formed than for the forward reaction (see Supplemental information and Fig. S3).

Different ratios of Sco to Cu_A

At a 1:1 ratio, the most reactive pair of mutants, Sco-Cys49:Cu_A-Cys153, appears to demonstrate a biphasic reaction mechanism consisting of an initial rapid increase in percent TNB followed a slower increase over time. In order to further characterize the MDI-forming mechanism, Sco-Cys49 and Cu_A-Cys153 were reacted at different ratios to determine what effect, if any, stoichiometry could have on the kinetics of the reaction (Fig. 4). When *Tt*Cu_A is in excess, less TNB is released overall compared to when the concentrations of the proteins are equimolar or *Tt*Sco is in excess. In the 1:0.5 reaction, with

Table I. *Percent TNB conjugated to and cysteine solvent accessibility for* Tt*Sco and* Tt*Cu_A*

Protein	Average TNB conjugated (%)	Average solvent accessibility (range)[c]
*Tt*Sco-Cys 49[a]	69.5 ± 5.6	10% (0–55%)
*Tt*Sco-Cys 53[a]	53.5 ± 8.0	2% (0–10%)
TtCu_A-Cys 149[b]	69.0 ± 3.5	67% (50–100%)
TtCu_A-Cys 153[b]	83.6 ± 4.2	53% (0–94%)

[a]%TNB released after 10 min incubation with DTT
[b]% TNB released after 30 min incubation with DTT, TNB is from the conjugation during lysis.
[c]Determined using the GetArea[34] program for each of the models from the NMR structure for Sco (2K6V) and apo Cu_A (2LLN).

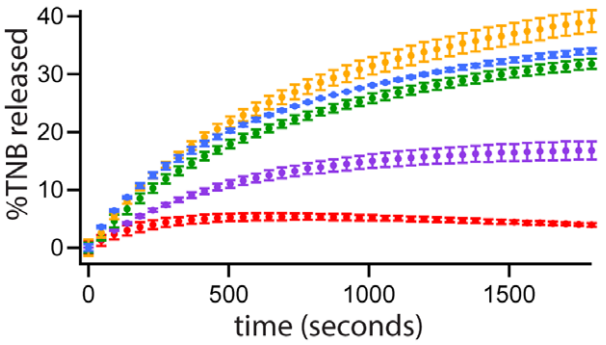

Figure 4. MDI reaction ratios. Percent TNB released from *Tt*Cu_A-Cys153 upon reaction with *Tt*Sco-Cys49 at different stoichiometric ratios. Yellow: 1.2:1 *Tt*Sco:*Tt*Cu_A, Blue: 1.4:1, Green: 1:1, Purple, 1:0.75, Red, 1:0.5.

TtCu_A in excess by a factor of 2, the amount of TNB released reached a peak before the signal began to slowly decrease. However, in the 1:0.75 reaction when the ratio is in excess by 1.33, the percentage of TNB released reached an asymptote. For reactions where the proteins are combined at a 1:1 ratio and above, percent TNB release continues to slowly increase over time displaying biphasic kinetics. Upon further analysis (see Supplemental information), the source of this biphasic nature stems from the fact that TNB that is released upon MDI formation appears to be able to react with other thiol containing species. This reaction in the solution produces newly conjugated molecules (Figs. S4 and S5). These other molecules then can slowly release the TNB over time, resulting in the "slow" step observed (Fig. 4).

Finding the roles of His 139 and Arg 48

Another residue that has been implicated in the proposed function of Sco in Cu_A assembly is the conserved histidine found in all Sco proteins. In *Tt*Sco, this is *Tt*Sco-His139 and this histidine is proposed to bind metal ions. In this study, the role of *Tt*Sco-His139 in MDI formation was studied through the creation of a double mutant, ScoC53S/H139A (Sco-Cys49/Ala 139), one that maintained the most reactive Cysteine 49 of *Tt*Sco while removing the less reactive thiol of Cysteine 53 and mutating histidine 139 to an alanine residue. When the Sco-Cys49/Ala 139 double mutant and Cu_A-Cys153 were reacted at a 1:1 ratio, TNB release was observed, indicating that the loss of *Tt*Sco-His139 does not prevent formation of the MDI [Fig. 5(A)]. Additionally, the kinetics of the Sco-Cys49/Ala139:Cu_A-Cys153 MDI forming reaction are similar to those of the Sco-Cys49:Cu_A-Cys153 combination, displaying a slow increase in percent TNB release over time. Thus, removing His139 does not appear to greatly affect the disulfide attack between the two proteins.

Adjacent residues to those that perform a nucleophilic attack can affect the nucleophilic activity. In

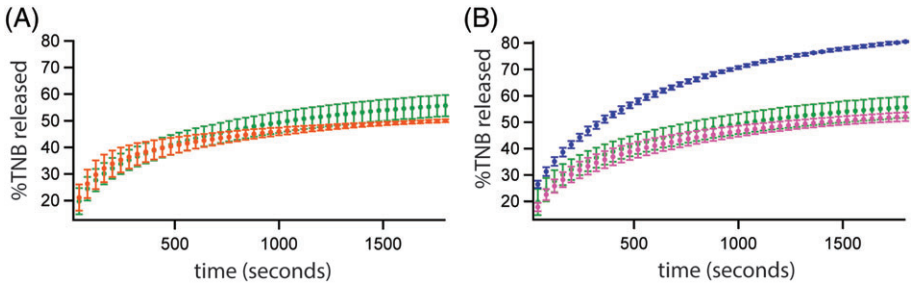

Figure 5. MDI reaction formed by different *Tt*Sco mutants at 1:1 *Tt*Sco:*Tt*Cu_A ratio. (A) Percent TNB released from *Tt*Cu_A-Cys153 upon reaction with either *Tt*Sco-Cys49 (green) or *Tt*Sco-Cys49/Ala139 (red-orange). (B) Percent TNB released from *Tt*Cu_A-Cys153 upon reaction with *Tt*Sco-Cys49 (green), *Tt*Sco-Cys49/Ala48 (pink) or *Tt*Sco-Cys49/Asp48 (dark blue).

*Tt*Sco, arginine 48 is adjacent to Cysteine 49. To test the effect of amino acid 48, two mutants were created that changed the positively charged arginine to alanine Sco-Cys49/Ala 48 (Sco R48A/C53S) or aspartate Sco-Cys49/Asp48 (Sco R48D/C53S). The MDI formation with this mutant was monitored using a 1:1 Sco:Cu_A ratio [Fig. 5(B)]. An alanine in Position 48 does not appear to change the amount of MDI formed appreciably. However, placing an aspartate next to the cysteine does increase the amount of MDI. One possible explanation is that putting the negatively charged aspartate adjacent to the reactive thiol incurs a H^+ transfer from cysteine to the aspartate to create an aspartic acid and a cysteine thiolate. The thiolate would be much more reactive than the thiol. There are also several polar residues near Cu_A-Cya153 and the Asp may form stabilizing interactions with them that help drive MDI formation. Clearly, an Asp at residue 48 does directly affect the formation of MDI unlike the putative metal ligand H139.

Role of metal ions

While the thiol reaction is evident in this system, a very important question remains about the role of metal binding in Sco activity. Sco from several organisms has been shown to bind Cu^{2+} and Cu^{1+} *in vitro*, with Cu^{1+} thought to bind *in vivo*.[1,26,27,32,33] We have found that *Tt*Sco will bind Cu^{2+}, Co^{2+}, Cd^{2+}, and Ni^{2+} with varying affinities (Shaw, Hunsicker-Wang et al. manuscript in preparation). To begin to address the role of metals in Sco activity, Cu^{2+}-bound Sco was reacted with TNB-labeled *Tt*Cu_A. No TNB release was detected (Fig. S6) when the UV–visible reaction was performed. In fact, a decrease in the absorbance at 412 nm over time was noted, which may result from the copper ions interacting with the TNB. To clarify the products yielded by the reaction, a time course experiment that utilized SDS PAGE gels run in the absence of DTT were performed. The reaction without metal ions was also performed to compare. When no copper is bound to Sco, the MDI is formed over the course of the 30 min [Fig. 6(A)]. However, when Cu^{2+} is bound to Sco-Cys49 (Sco-Cys49-Cu^{2+}) before incubating with Cu_A-Cys153, only a minor amount of MDI is formed over the course of 30 min [Fig. 6(B)]. Thus, it appears that Cu^{2+} binding greatly diminishes the formation of MDI. Since Sco is proposed to bind Cu^+ *in vivo,* the reaction was repeated with Cu^+ bound to Sco-Cys49 (Sco-Cys49-Cu^{1+}). No detectable MDI was formed in any of the experiments indicating that Cu^{1+} bound to Sco *precludes* MDI formation. The small amount of MDI formed with the Cu^{2+}-bound Sco could be due to a lower relative affinity of Cu^{2+} to Cu^{1+} for *Tt*Sco. Thus, the weaker interaction may result in a faster off rate, resulting in more apo-Sco which could be reactive with Cu_A.

Based on all these data, according to the mechanism of thiol-disulfide oxidoreductases (Fig. 2), it is *Tt*Sco Cysteine 49 that attacks the disulfide bond in *Tt*Cu_A. The new bond that is formed connects to *Tt*Cu_A Cysteine 153. These results indicate that the disulfide reduction mechanism proceeds through a mixed disulfide intermediate and that these two cysteines are the "reactive" pair that forms the MDI in the first step of this mechanism. The lower amounts of TNB released by other combinations of mutants (besides that of Sco-Cys 49 with Cu_A-Cys153) indicate that the reduction of *Tt*Cu_A by *Tt*Sco is a specific reaction which proceeds through the interaction of a unique combination of cysteines. The reaction is reversible and the extent of MDI formation depends on the ratio of Sco to Cu_A. Loss of the conserved histidine via the mutation of *Tt*Sco-Cys49/Ala139 also appears to have little effect on MDI formation, whereas tuning of the reactive cysteine by the neighboring Arginine 48 (*Tt*Sco-Cys49/Ala48 or *Tt*Sco-Cys49/Asp48) does alter the formation of MDI. The binding of Cu^{2+} appears to diminish the formation of the mixed disulfide intermediate and Cu^{1+} precludes formation and thus may stop the disulfide bond reducing activity in general.

Discussion

Sco Cysteine 49 is the thiolate that attacks the disulfide bond in the apo-*Tt*Cu_A protein and the increased reactivity of this cysteine could stem from two causes. First, *Tt*Sco Cysteine 49 samples more positions, as

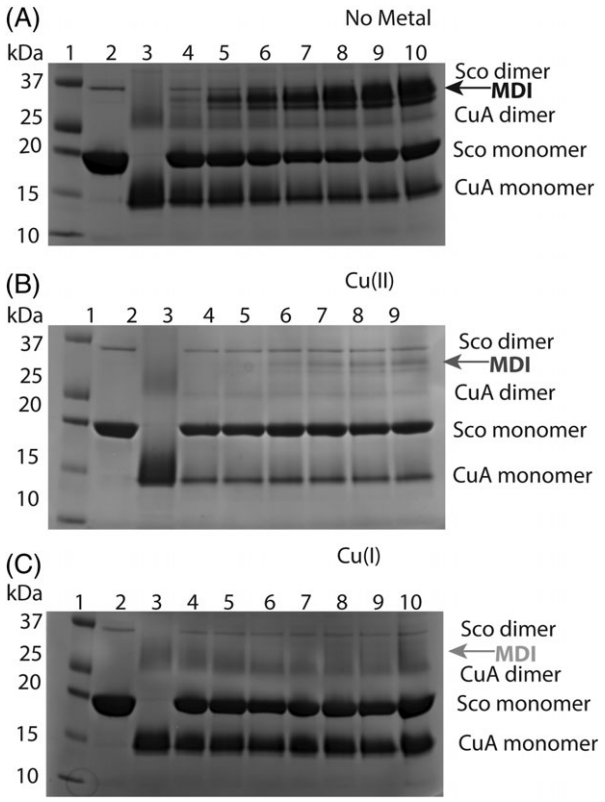

Figure 6. Comparison of *Tt*Sco-Cys49 reaction with *Tt*Cu_A-Cys153 to metal-bound *Tt*Sco-Cys49. SDS-PAGE gels run in the absence of DTT of each reaction. All of the time course reactions were quenched with MMTS at the designated time. Labels and arrow on the right indicates the species that are possibly present. (A) *Tt*Sco-Cys49 reaction with *Tt*Cu_A-Cys153 Lane 1 MW ladder, Lane 2 *Tt*Sco-Cys49 Lane 3 *Tt*Cu_A-Cys153, Lane 4 *Tt*Sco-Cys49: *Tt*Cu_ACys153 at 0 min, Lane 5 at 2 min, Lane 6 at 5 min, Lane 7 at 10 min, Lane 8 at 20 min, Lane 9 at 30 min, Lane 10 after more than 40 min. (B) *Tt*Sco-Cys49-Cu^{2+} reaction with *Tt*Cu_A-Cys153 (Cu^{2+} bound to Sco prior to incubation with Cu_A) Lane 1 MW ladder, Lane 2 *Tt*Sco-Sco:*Tt*Cys49-Cu^{2+} Lane 3 *Tt*Cu_ACys153, Lane 4 *Tt*Sco-Cys49-Cu^{2+}: *Tt*Cu_A-Cys153 at 0 min, Lane 5 at 2 min, Lane 6 at 5 min, Lane 7 at 10 min, Lane 8 at 20 min, Lane 9 at 30 min. (C) *Tt*Sco-Cys49-Cu^{+}: *Tt*Cu_ACys153 (Cu^{+} bound to Sco prior to incubation with Cu_A) Lane 1 MW ladder, Lane 2 *Tt*Sco-Cys49-Cu^{+}, Lane 3 *Tt*Cu_ACys153, Lane 4 *Tt*Sco-Cys49-Cu^{2+}: *Tt*Cu_ACys153 at 0 min, Lane 5 at 2 min, Lane 6 at 5 min, Lane 7 at 10 min, Lane 8 at 20 min, Lane 9 at 30 min, Lane 10, after more than 40 min.

evidenced by the number of positions found in the 31 models of the NMR structure (PDB 2K6V) (Fig. 7).[3] This lack of constrained geometries is likely due to the fact that it is found on a non- or less structured portion of the protein, whereas Sco Cysteine 53 is found at the N-terminal end of an α-helix. The secondary structure of Sco cysteine 53 likely prohibits the amino acid from sampling more positions. A calculation of the solvent accessibility of these amino acids over the 31 structures in the solution structure[4] using the program GetArea[34] gave an average of 10% solvent exposed (range 0–37%) for Sco Cysteine 49, whereas Sco Cysteine 53 was an average of 2% solvent exposed (range 0–10%) (Table I). The flexibility of these regions of the proteins likely influence the solvent accessibility and thus the cysteine with more solvent exposure also has the greatest range of positions.

In the apo *Tt*Cu_A structure (PDB 2LLN),[35] both Cysteine 153 and Cysteine 149 are "solvent exposed." Interestingly, using the same treatment as for *Tt*Sco, the solvent exposure of *Tt*Cu_A Cysteine 153 is found to be 53% solvent exposed (range 0–94%) and *Tt*Cu_A Cysteine 149 is 67% (50–100%). Thus, unexpectedly, the average solvent exposure of Cysteine 149 is higher; however, the range of solvent exposure is less than for Cysteine 153. Thus, in the case of Cysteine 153, the fewer geometric constraints in the NMR structure of the site where Cysteine 153 is located may be more important. Cysteine 153 is found in a loop whereas Cysteine 149 is found at the end of a β strand in the holo protein structure.[36] In addition, the two amino acids to the N-terminal side of Cysteine 149 are both isoleucine, which may make the Cysteine 149 less susceptible to nucleophilic attack because the negative charge would be less stable in the more hydrophobic environment around that cysteine. Indeed, the structural analysis of the apo Cu_A protein by Vila et al. show that the all of the residues around the metal binding region are not well defined and suggest some degree of flexibility.[35] Thus in both *Tt*Sco and *Tt*Cu_A the less constrained cysteine is the one involved in the highest amounts of MDI formation.

The amino acid adjacent to Sco Cysteine 49 in *Tt*Sco is an arginine. In Sco proteins, the amino acid

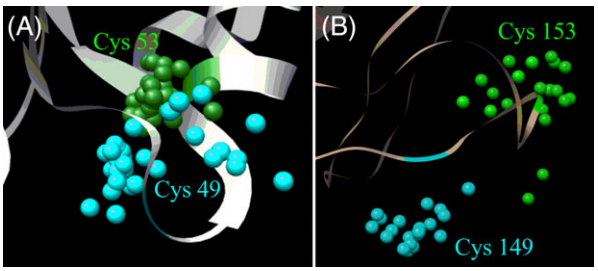

Figure 7. The positions of cysteine residues in *Tt*Sco and *Tt*Cu_A. (A) The positions of Cysteine 53 versus Cysteine 49 in *Tt*Sco in the NMR solution structure. The spheres are the S atoms of the cysteine residues found in the 31 different models in the NMR structure of *Tt*Sco. Only the spheres are shown for clarity. Cysteine 53 positions are shown in green, Cysteine 49 positions are shown in cyan, and the ribbon diagram is Model 1 of the NMR structure (2K6V).[3] B) The positions of Cysteine 153 versus Cysteine 149 in apo *Tt*Cu_A in the NMR solution structure. The spheres are the S atoms of the cysteine residues found in the 20 different models in the NMR structure of *Tt*CuA. Only the spheres are shown for clarity. Cysteine 153 positions are shown in green, Cysteine 149 positions are shown in cyan, and the ribbon diagram is Model 1 of the NMR structure (2LLN).

that is one step toward the N-terminal side is varied, but is often histidine, asparagine, or lysine[11,17,22] *Escherichia coli* thioredoxins have cysteines with differential pK_a values and reactivities and generally have charged residues near the cysteine residues.[37,38]

The periplasmic thioredoxin-like protein TlpA, from the bacteria *Bradyrhizobium japonicum* has been shown to reduce both the Sco1 protein and the Cu_A site cysteines.[39] TlpA attacks the more N-terminal cysteine in the Cu_A site. In our *Tt*Sco system, the more C-terminal Cysteine in Cu_A is attacked. Interestingly, when TlpA attacks Sco1, it is the more C-terminal cysteine that is attacked. Thus, there is likely site complementarity determining which cysteine is reactive and which cysteine is attacked in each of these systems.

As with any *in vitro* system, it is possible that the activity of the protein may differ *in vivo.* In this system, there are differences due to the absence of the transmembrane helix anchoring Sco to the membrane and the use of the TNB-protein S–S bond instead of a protein disulfide bond. The reduction potential of the TNB-protein disulfide may therefore differ and have an effect on the reaction, although it is likely that the existence of the functionality *in vitro* mirrors that of the *in vivo* reaction.

The data presented here only begin to elucidate why *Tt*Sco binds metal. Indeed, *Tt*Sco does bind several divalent metals including Cu^{2+}. (Shaw, Hunsicker-Wang et al., manuscript in preparation). [3] The result that the binding of Cu^{2+} or Cu^{1+} to the mutant Sco precludes or greatly diminishes MDI formation may indicate a regulatory role, or that it may force the protein to transfer any bound metal to a specific partner before it can perform the disulfide bond reduction. While the two cysteines of Sco's conserved CXXXC motif are implicated in both copper binding and disulfide bond reduction, this may not be the case for the proximal conserved histidine. Although *Tt*Sco-His139 is also implicated in metal binding, the loss of this histidine via the H139A mutation does not appreciably affect MDI formation in this system (Fig. 5). However, in *Bacillus subtilis* Sco (*Bs*Sco), the analogous His135 is a copper ligand, and the analogous *Bs*H135A mutation abrogates assembly of COX, suggesting that it plays a role in the function of *Bs*Sco.[40] With Sco-Cys49/Ala139, the formation of the MDI was not halted. The kinetics plots of MDI formed by the single mutant versus that of the double mutant do display similar shapes. With the analogous mutation in *Bs*Sco, H135A, oxidation rates of exogenous reductants increased, suggesting that the histidine is implicated in some redox-related role, potentially that of a redox sensor.[40] As a result, it was expected that with the Sco-Cys49/Ala 139 mutant, some change would be observed and thus it must be recognized that variations in the role of the conserved histidine may be simply due to difference between the species of bacteria. Thus, the exact role of this metal binding and its tie to the disulfide bond reduction remains an interesting question still to be answered.

In this study, we present one possible hypothesis that could reconcile some of the different observations in the *T. thermophilus* system. Since *T. thermophilus* has only one Sco, perhaps *Tt*Sco also delivers a copper ion to another site, the Cu_B site. The *T. thermophilus* system lacks a Cox11 protein, which is thought to deliver the copper to the Cu_B site in *S. cerevisiae* and *R. sphearoides* systems.[16,41] Previous studies have pointed to Sco delivering copper to the Cu_B site in the cbb_3 systems, which lack a Cu_A site but still have a Sco protein expressed.[42,43] In this theoretical possibility, the *Tt*Sco is bound with copper, which precludes the reduction of the Cu_A site. Once, the copper is delivered to the Cu_B site, then *Tt*Sco, which remains reduced, is liberated to perform an attack on the disulfide bond in the Cu_A site, proceeding through the MDI and resulting in reduced Cu_A, which is then metallated by PCu_AC, as shown previously.[3] The hypothesis is untested, but fits with the MDI formation data presented in this study and previous studies.[3]

Due to the varied function and specificity displayed by Sco,[12,13] this hypothesis may only be applicable to the *Thermus thermophilus* Sco. For example, in the Sco protein from *Bacillus subtilis*, the Cu^{2+} state of the protein is necessary for maturation of the cytochrome caa_3 oxidase,[28,29] and the *Bacillus* system also does not show formation of MDI. These results further demonstrate that the findings from one system may or may not be applicable to other species and may bring to light insightful divergences in the evolution of cytochrome oxidase assembly. The *T. thermophilus* only has one Sco, whereas many other systems have both a Sco1 and Sco2, which divide disulfide bond reduction activity and metal binding.[16,22,30] *Thermus thermophilus* has a separate copper binding protein, PCu_AC, that delivers the copper ions to the Cu_A site.[3]

Conclusions

The function of Sco is still to be determined unambiguously, but in the case of *T. thermophilus* Sco, there is mounting evidence of its role, or just as likely, one of its roles as a thiol-disulfide oxidoreductase.[3] The data presented here uphold that role for this specific Sco protein, *Tt*Sco, expand on a mechanism by which the disulfide bond reduction can occur and establish that Cu^{2+} binding stops the reaction from occurring. It has also been suggested that Sco proteins from other species can act in different roles and/or have multiple roles (cf. Refs. [4,7,8,13,22,28,29,42,44]) Thus, continued study is certainly needed to fully understand this fascinating protein.

Materials and Methods

The gene for the Sco protein was kindly provided by Denis Winge to J. A. Fee who then provided the Sco gene in a pET24b plasmid to this lab. In order to add a purification tag and increase yield, a Ligation Independent Cloning (LIC) vector, pET-30 Ek/LIC (EMD Biosciences) was chosen. For LIC cloning, Sco was PCR amplified using the primers below:

ScoLICF: 5′GACGACGACAAGATGCTTCCCCG GGGGCAC3′.

ScoLICR: 5′GAGGAGAAGCCCGGTTTAAAGAA GGGCCTG3′.

GC melt (Clonetech) and DMSO were added to the reaction mix [5 μL 10× Rxn buffer, 5ul GC melt, 2.5 μL DMSO, 1 μL DNA template, 1.25 μL F/R Primers, 1 μL dNTP, 1 μL Taq polymerase]. The product was then T4 DNA polymerase treated [10 μL PCR product, 2 μL 10× T4 DNA Pol Buffer, 2 μL 25 m*M* dATP, 2ul 100 m*M* DTT, 4.6 μL water and 0.4 μL T4 DNA polymerase] and incubated at 22°C for 30 min and then 75°C for 20 min. Two microliter of the product was then annealed into 1ul pET30 Ek/LIC vector for 5 min at 22°C.

The product was checked on a 1% agarose gel, and then transformed into Novablue competent cells using a standard heat shock procedure. Plasmid preps (QIAprep Spin Miniprep kit) from the resulting colonies were used to sequence the plasmids, and determine which ones had a perfect Sco insert. Primers for sequencing were T7 promoter primers. These plasmids were then transformed using the same heat shock procedure, into Novagen BL21 (DE3) competent *E. coli* cells. Cultures were then grown in standard LB broth with added 10 mg/ml kanamycin. The cultures were grown either as uninduced, or induced at OD = 1.0 with 0.3 m*M* IPTG. The cells were spun down and frozen at −80°C for storage. A glycerol stock was also made of each positive colony. This construct (Fig. S1) is slightly different than the construct used in a previous study.[3] The *Tt*Cu_A vector used here is also different than what was used previously[45] in that the protein is in a pET17b vector containing an ampicillin resistance gene. The mutants were made from these vectors.

Mutants of TtSco and TtCu$_A$

The mutations *Tt*Sco and *Tt*Cu_A were made using the Agilent Quikchange or Quikchange II kit. The following primers and their reverse compliments were used to make the cysteine to serine mutations (mutations are underlined and bold face): Sco-Cys53 (C49S): 5′GGCTTCACCCGC**A**GCCCCGACGTCTG3′.

Sco-Cys49 (C53S): 5′CTGCCCCGACGTC**A**GCCC CACCACC3′.

Cu_A-Cys153 (C149S): 5′GAGTACCGCATCATC**A** GCAACCAGTACTGCG3'.

Cu_A-Cys149 (C153S): 5′CTGCAACCAGTAC**A**GC GGCCTAGGCCAC3′.

Sco-Cys53 is the *Tt*Sco mutant Sco-C49S; Sco-Cys49 is the *Tt*Sco mutant C53S; Cu_A-Cys153 is the *Tt*Cu_A mutant C149S, and Cu_A-Cys149 is the *Tt*Cu_A mutant C153S.

The double mutants were produced using the Sco C53S plasmid as the parent plasmid and the following primers to produce the double mutants. All resulting vectors were sequenced to confirm the presence of the mutations.

Sco-Cys49/Ala 139 (C53S/H139A): 5′GAGTACCT GGTGGAC**GC**CACCGCCACCACCTTC 3′.

Sco-Cys49/Ala 48 (R48A/C53S): 5′CTTCGGCTTC ACC**GC**CTGCCCCGACGTC3′.

Sco-Cys49/Asp 48 (R48D/C53S): 5′CTTCGGCTT CACC**GA**CTGCCCCGACGTC3′.

Sco-Cys49/Asp 48 (R48D/C53S): 5′CTTCGGCTT CACC**GA**CTGCCCCGACGTC3′.

The presence of the mutations, or double mutations, in the protein was checked by confirming the intact mass of the proteins at either Trinity University or at the mass spectrometry core at the University of Texas Health Science Center. At Trinity University, mass spectra were acquired in positive ion mode on an Agilent 6230 electrospray ionization time-of-flight mass spectrometer. The intact protein mass data were deconvoluted with a maximum entropy algorithm using Agilent MassHunter BioConfirm software. See Figure S7 for example mass spectrometry data for Sco-Cys49/Ala 139 and Sco-Cys49/Ala48.

Growth and purification of TtSco

Plasmid containing the mutant or double mutant gene was transformed into BL21(DE3) cells according to the manufacturer's protocol, plated onto LB agar plates containing 100 μg/mL kanamycin, and grown overnight at 37°C. A single colony was used to inoculate a 5 mL culture in the presence of 100 μg/mL kanamycin at 37°C and was grown for approximately 3 h. The 5 mL culture was then used to inoculate a 250 mL culture and the cells were induced at an OD_{600nm} of 1.0 with IPTG at a final concentration of 0.4 m*M*. After induction, the temperature was dropped to 30°C and the cells were allowed to grow overnight. The cells were collected by centrifugation for 5 min at 5000*g* and 4°C. The cells were resuspended in Tris pH 8.0 (25 mL/1 L bacterial culture). The cells were lysed by addition of 4 mg/mL lysozyme, 40 units/mL DNAse, 3 units/mL RNAse, 0.1% Triton, and enough PMSF to reach a final concentration of 2 m*M*. A protease cocktail (Thermo Fisher, Halt) was also added to the solution. In addition, 1.4 m*M* methyl methanethiosulfonate (MMTS) (Thermo Fisher Scientific, Pierce) was added in order to block the remaining cysteine thiol from forming Sco dimers and reacting with other thiol-containing

biomolecules in the lysis solution. The lysis was stirred for an hour at room temperature and then centrifuged at 12,000*g* for 15 min at 4°C.

The filtered cell lysate (2 mL) was placed over a 5 mL His-Trap Ni-NTA FPLC column (GE Healthcare) at 8°C. The column was run using a linear gradient between 10% of the elution buffer (50 m*M* sodium phosphate, 300 m*M* NaCl, 500 m*M* imidazole, 0.05% Tween, pH 7.0) to 75% (4.4%/column volume). The protein purity was verified by analyzing the fractions on a 12% MOPS NuPAGE SDS-PAGE run following the manufacturer's protocol (Life Technologies) except that the proteins are heated to 90°C for 10 min. The pure fractions were placed in dialysis overnight (2 × 1 L of 10 m*M* sodium phosphate, 0.05% Tween, pH 7.0). The histidine purification tag was removed following the manufacturer's protocol using Enterokinase (EK) (MilliporeSigma) except that 0.1 units of EK/0.2 mg of protein were used. The mixture was rocked at room temperature for 16 h. The EK was removed using an EK-Away Kit (Life Technologies). To remove the purification tag from the protein sample, the solution was placed back over the Ni-NTA column equilibrated using the same conditions that obtained pure tagged protein. Pure untagged-*Tt*Sco was present in the flow through. The purity of untagged-*Tt*Sco was verified by analyzing the flow through on a 12% MOPS NuPAGE SDS-PAGE run following the manufacturer's protocol (Life Technologies). Purity was assessed by the presence of untagged *Tt*Sco at 19 kDa with no other major species present. Pure untagged-*Tt*Sco was placed in dialysis overnight (10 m*M* Tris, 0.05% Tween, pH 8.0) and changed once.

TtCu$_A$ growth and purification

BL21(DE3) cells were transformed with the ampicillin resistant *Tt*Cu$_A$ mutant plasmid, Cu$_A$-Cys153 or Cu$_A$-Cys149. Cells were grown on plates with 100 μg/mL ampicillin at 37°C overnight. A single colony was used to inoculate a 5 mL culture that was grown overnight. The 5 mL culture was used to inoculate 1 L of LB broth, which contained 100 μg/mL ampicillin and the culture was grown at 37°C. When the OD_{600nm} reached 1.0 the cells were induced with IPTG at a final concentration of 0.2 m*M*. Cells were allowed to induce for a total of 5 h, then harvested at 5000*g* for 5 min, decanted, and frozen at −80°C. The protein was purified similarly to what was previously published.[45] The cell pellet from a 1 L culture was lysed with 50 m*M* Tris pH 8.0, 100 mg lysozyme, 1000 units DNAse, 75 units RNAse, 0.1% Triton, and 2 m*M* PMSF. The cells were incubated at room temperature for 1 h and centrifuged at 12,000*g* for 15 min. The supernatant was treated with a 65°C water bath for 10 min and then centrifuged at 12,000*g* for 30 min. The pH of the supernatant was adjusted to 4.6 and cooled on ice for 30 min, after which it was centrifuged again at 12,000*g* for 30 min. A 20 mL volume of 5 m*M* 5,5′-dithiobis-(2-nitrobenzoic acid) (Ellman's reagent, DTNB) in 500 m*M* phosphate, pH 7.5 was added to the supernatant in order to conjugate a 2-nitro-5-thiobenzoate (TNB) to the free thiol. The conjugated protein was dialyzed overnight (2 × 1 L) in 50 m*M* sodium acetate, 0.02% Tween, pH 4.6.

The sample was then purified using a room temperature, gravity CM (GE Healthcare) cation exchange column equilibrated with 50 m*M* sodium acetate, 0.02% Tween, pH 4.6, and eluted with 50 m*M* sodium acetate, 1 M sodium chloride, 0.02% Tween, pH 4.6 using a very shallow, 1 L gradient. The fractions that contained the *Tt*Cu$_A$ protein were determined using MOPS NuPAGE SDS gels (Life Technologies). The fractions were pooled and dialyzed overnight into 2 x 1 L 50 m*M* sodium acetate, 0.02% Tween, pH 4.6. After dialysis, the samples were further purified using a 5 mL SHP cation exchange column (GE Healthcare) equilibrated with 50 m*M* sodium acetate, 0.02% Tween, pH 4.6 and were eluted with 50 m*M* sodium acetate, 1 M sodium chloride, 0.02% Tween, pH 4.6. Again, the gradient was very shallow (0.26%/ CV). If the protein was not pure after this column, the samples further separated using a Superdex 75 (GE Healthcare) size exclusion column using 50 m*M* sodium acetate, 0.02% Tween, pH 4.6 as buffer. The final protein purity was determined using MOPS NuPAGE SDS gels (Life Technologies), and the protein was stored at −20°C.

Mixed disulfide intermediate formation at 1:1 ratio

UV–visible measurements were performed on a Hitachi U2800 or U3000 spectrophotometer. The mixed disulfide intermediate was trapped because the adjacent thiols needed to complete the reduction mechanism have been removed (Fig. 2). The reaction was performed in 10 m*M* Tris, pH 8.0, 0.05% Tween. *Tt*Sco mutants were reduced (which also removes the -S-CH_3 protection group) using a 10-fold excess of dithiothreitol (DTT) and allowed to incubate for 1 h. Following reduction, the DTT was removed with PD-10 desalting columns (GE Healthcare). The reduced *Tt*Sco was subsequently reacted with TNB-conjugated *Tt*Cu$_A$ at a 1:1 ratio using 60 μM concentrations at room temperature within 1 h of being reduced. The reaction was monitored over time at 412 nm, corresponding to the absorbance of TNB (ε = 14150 M^{-1} cm^{-1}).[46] The reaction was monitored for 30 min and the products were quenched using a 10-fold excess of MMTS. Both reducing (with DTT) and non-reducing gels (without DTT) were used to analyze the products formed and to test for the presence of disulfide linkages (Fig. 3). DTT was added to a separate sample of *Tt*Cu$_A$ to determine the maximum value that could be reached for that sample at 412 nm, in order to calculate the % TNB released.

Mixed disulfide intermediate formation at non-1:1 ratios

The MDI formation was performed as for the 1:1 ratios except that the reduced TtSco was subsequently reacted with TNB-conjugated *Tt*CuA at room temperature at various concentrations (84 μM, 75 μM, 45 μM, 30 μM) within 1 h of being reduced.

%T TNB conjugation to pure protein

Sco-Cys49 and Sco-Cys53 were reduced in an anaerobic environment (glove bag inflated with N_2) by adding a 10× molar excess of DTT and left to sit for 1 h. To remove excess DTT, the reduced Sco was passed over a PD-10 column and eluted in 1 mL fractions using 10 m*M* Tris, 0.05% Tween, pH 8.0. Fractions containing Sco were combined and quantified at which point 10× molar excess DTNB was added. This reaction sat for 1 h to allow TNB to conjugate to Sco. The reaction was then removed from the glove bag. Excess DTNB was removed by dialyzing into 10 m*M* Tris pH 8.0 and 0.05% Tween overnight. Sco was re-quantified after dialysis. Sixty micromolar of Sco was then added to a quartz cuvette and placed in the UV–visible spectrophotometer. Ten microliter of 25 m*M* DTT was quickly added and the absorbance at 412 nm was monitored for 10 min to measure the release of TNB. The final value at 412 nm was divided by the absorptivity (14,150 cm^{-1} M^{-1}) to find the concentration of TNB released. This value was divided by 60 μM to find the percentage of TNB conjugated to the protein originally.

"Role reversal"

The set up for the "role reversal" experiment required conjugation of TNB to the purified Sco in order to produce the reaction target as well as reduction of Cu_A in order to yield the nucleophilic species. The TNB labeled Sco, Sco-Cys49, or Sco-Cys53 was produced as described above. The Cu_A mutants were reduced to remove the conjugated TNB using a 10-fold excess of DTT. The protein and DTT were allowed to incubate for 1 h. Following reduction, the DTT and TNB were removed with PD-10 desalting columns (GE Healthcare). Subsequently the experiment was performed in the same fashion as the "Mixed disulfide intermediate formation at 1:1 ratio" trials. The reduced Cu_A was reacted with TNB conjugated Sco at a 1:1 ratio using 60 μM concentrations. The reaction was monitored by UV–visible spectroscopy at 412 nm corresponding to free TNB in solution, as described above.

Sco-TNB anaerobic conjugation

Sco-Cys49 was reduced in an anaerobic environment (glovebox inflated with N_2/H_2) with 10× molar excess DTT and left it to sit for 1 h. To remove excess DTT, the reduced Sco was placed over a PD-10 column (GE Healthcare) and eluted in 1 mL fractions using 10 m*M* Tris, 0.05% Tween, pH 8.0. Fraction 3 was kept and set aside. DTNB [5,5′-dithiobis-(2-nitrobenzoic acid)] was also reduced in an anaerobic environment with 10× molar excess DTT and left to sit for 30 min. Reduced DTNB was passed over another PD-10 column and eluted into 1 mL fractions using 10 m*M* Tris, 0.05% Tween, pH 8.0 buffer. The darkest yellow fraction, containing the now-reduced TNB, was kept and set aside. Reduced Sco Fraction 3 was combined and mixed with the darkest reduced TNB fraction and left to sit in anaerobic conditions for over 20 minutes to allow for conjugation of TNB to Sco. The Sco-TNB mixture was then placed over a third PD-10 column and eluted into 1 mL fractions using 10 m*M* Tris, 0.05% Tween, pH 8.0 buffer. UV–visible measurements (Hitachi U2800) were used to verify the presence of a Sco-TNB conjugate in the fractions. UV–Visible spectra of each fraction were taken from 200–500 nm. The presence of signals at 320–330 nm suggested the presence of a Sco-TNB conjugate (412 nm suggested free TNB). Fractions possessing these signals were quantified using the Edelhoch method. The Sco-TNB fractions were diluted to a final concentration of 60 μM in a quartz cuvette using 10 m*M* Tris, 0.05% Tween, pH 8.0. One microliter of 500 m*M* DTT was added to the cuvette, the cuvette was inverted to mix, and a spectrum was taken from 200 to 500 nm to monitor release of TNB. An increase at 412 nm indicated the presence of free TNB, and a decrease at 320–330 nm indicated a decrease in the Sco-TNB conjugate.

Sco-Cys49/Ala 139, Sco-Cys49/Ala 48, Sco-Cys49/Asp48 growth and purification

The Sco double mutants were grown and purified following the same protocol as the Sco-Cys53 and Sco-Cys49 mutants except that these mutants required further purification. After verifying the removal of the tag as reflected by a change in molecular weight, the untagged double mutant was pooled and placed into dialysis overnight (10 m*M* Tris, 0.05% Tween, pH 8.0) and changed once. The untagged-*Tt*Sco was then placed over a 5 mL SHP cation exchange column (GE Healthcare) at 8°C equilibrated with 50 m*M* sodium acetate, 0.02% Tween, pH 4.6 and eluted with 50 m*M* sodium acetate, 1 M sodium chloride, 0.02% Tween, pH 4.6. Protein purity was determined using MOPS NuPAGE SDS gels (Life Technologies).

Sco-Cys49/Ala 139, Sco-Cys49/Ala 48, Sco-Cys49/Asp48 mixed disulfide intermediate formation

These experiments were performed in the same fashion as the "Mixed disulfide intermediate formation at 1:1 ratio" trials.

Cu^{2+} binding to Sco-Cys49 and subsequent reaction with Cu_A-Cys153 (UV–visible experiment)

For all metal binding and subsequent MDI experiments, the proteins were exchanged into the metal binding buffer (10 m*M* phosphate and 0.05% Tween pH 7.0) using dialysis or a PD-10 column. Sco-Cys49 was reduced with a 10-fold excess of dithiothreitol (DTT) in an anaerobic environment. After 1 h, protein was passed over a PD-10 column and eluted in 1 mL fractions using 10 m*M* phosphate and 0.05% Tween pH 7.0. The concentration of the reduced protein was determined using the Edelhoch method[47] (absorbance at 280 nm, molar absorptivity of 8995 M^{-1} cm^{-1}). The UV–visible spectrum was obtained and then Cu^{2+} ($CuSO_4$) was bound in a 1:1 fashion. After binding, a UV–visible spectrum was taken once more to ensure the presence of the characteristic 358 nm charge transfer band. The metal bound protein was then used to react with the TNB-labeled Cu_A-Cys153 as performed for the "Mixed disulfide intermediate formation at 1:1 ratio" protocol above.

Cu^{1+} or Cu^{2+} binding to Sco-Cys49 and subsequent reaction with Cu_A-Cys153 (gel assay)

Both the Sco-Cys49 and Cu_A-Cys153 were exchanged into the metal binding buffer, 10 m*M* sodium phosphate buffer, 0.05% Tween, pH 7.0 using a PD10 column. The proteins were then quantified using the Edelhoch method described above.

All proteins, buffers, and solutions were degassed using nitrogen gas before taking into a glove bag. The glove bag was made anaerobic by exchanging three times with nitrogen gas and then sealed with a clip. Any time the glove bag was opened to bring items in or out, it was exchanged three times again and all lids and caps were affixed.

Sco-Cys49 was reduced in the glove bag using a 10× excess of DTT and allowed to sit for 1 h in the closed bag. The protein was the put onto a PD10 column and eluted in 1 mL fraction using the metal binding buffer. The five eluted fractions were then quantified using the Edelhoch method. A fraction of the highest concentration was then chosen to use for the Cu(I)-MDI experiment. The Cu(I) solution was made by adding water to an epitube with the Cu(I) salt (tetrakis(acetonitrile)copper(I) hexafluorophosphate (Sigma-Aldrich)) to a concentration of 1 m*M*. The metal solution was then quickly diluted again such that a 1–2 μL could be added to the fraction of reduced Sco-Cys49 to have a 1:1 protein: copper ratio.

The Sco-Cys49-Cu^{1+} was then added to the Cu_A-Cys153 (with the TNB already conjugated) solution in a 1:1 ratio. Immediately, one aliquot (6.5 μL) was removed and quenched with 1 μL 35 m*M* MMTS (which is the 0 min time point). Aliquots were removed again after 2, 5, 10, 20, and 30+ min to capture the time course of the experiment. Once the samples were finished reacting, all samples were brought out of the glove bag. The quenched samples were then run on an SDS-PAGE gel without DTT as described above. The experiment was performed in duplicate each time and performed on two different days (giving a total of four replicates).

A similar time course for the Cu(II) experiment was also performed at two different times in duplicate, one time in the glove bag and one time in the air to compare to the Cu(I) experiment. The only difference for the Cu^{2+} experiment was that the Cu(II) sulfate was used. A 100 m*M* stock was made in water and then diluted to 1 m*M* for use in adding the metal to the reduced Sco. There was no detectable (qualitative) difference in the results in air versus anaerobic conditions.

Solvent accessibility calculations using GetArea

For both apo *Tt*Sco and for apo *Tt*Cu_A, the solvent accessibility of the cysteine residues was determined using the GetArea program.[34] In both cases, the solution structures were used (2K6V for *Tt*Sco and 2LLN for apo *Tt*Cu_A). Each, individual model was put into a separate PDB file which was then submitted to the program. The solvent accessibility calculation was made for each amino acid, and the value for the two different cysteines recorded. The values for either cysteine residues in the structure were averaged and then the range computed.

Supplementary Material

Supplementary material includes the sequence information for *Tt*Sco, the raw A_{412} data for MDI formation, the role reversal MDI %TNB graph and nonreducing gel, an analysis of MDI biphasic kinetics analysis using TNB conjugates, the UV–visible % TNB conjugation reaction using Cu^{2+} bound Sco, and example mass spectrometry data used to confirm protein mutagenesis.

Acknowledgments

This work was supported by Research Corporation (Cottrell College Science Award 7963), the Welch Foundation (W-0031 [Trinity Chemistry Department]), FASTER grant SURF- National Science Foundation DUE S-STEM Award 1153796 (for C. R. H.) and the Arnold and Mabel Beckman Foundation Beckman Scholars Award (for L. E.). The mass spectrometer was acquired and supported by the National Science Foundation (CHE-1726441). Stipends for L. D. H., C. S. H., N. M., and A. D. P. were provided in part by a grant from the Howard Hughes Medical Institute. Research supplies for L. C. L. were provided in part by Mach Family Student Research Fellowships. We would like to thank the late J.A. Fee and Ying Chen of the Scripps Research Institute for

the *Tt*Sco and *Tt*CuA plasmids. We would like to acknowledge Taylor Devlin for performing one set of MDI reactions and Dr Adam Urbach for help with the mass spectrometry data.

References

1. Horng Y, Leary SC, Cobine PA, Young FB, George GN, Shoubridge EA, Winge DR (2005) Human Sco1 and Sco2 function as copper-binding proteins. J Biol Chem 280: 34113–34122.
2. Horng YC, Cobine PA, Maxfield AB, Carr HS, Winge DR (2004) Specific copper transfer from the Cox 17 metallochaperone to both Sco1 and Cox11 in the assembly of yeast cytochrome c oxidase. J Biol Chem 279: 35334–35340.
3. Abriata LA, Banci L, Bertini I, Ciofi-Baffoni S, Gkazonis P, Spyroulias GA, Vial AJ, Wang S (2008) Mechanism of Cu_A assembly. Nat Chem Biol 4:599–601.
4. Banci L, Bertini I, Ciofi-Baffoni S, Kozyreva T, Mori M, Wang S (2011) Sco proteins are involved in electron transfer processes. J Biol Inorg Chem 16:391–403.
5. Banci L, Bertini I, Ciofi-Baffoni S, Leontari I, Martinelli M, Palumaa P, Sillard R, Wang S (2007) Human Sco1 functional studies and pathological implications of the P174L mutant. Proc Natl Acad Sci USA 104:15–20.
6. Banci L, Bertini I, Calderone V, Ciofi-Baffoni S, Mangani S, Martinelli M, Palumaa P, Wang S (2006) A hint for the function of Sco1 from different structures. Proc Natl Acad Sci USA 103:8595–8600.
7. Leary SC, Sasarman F, Nishimura T, Shoubridge EA (2009) Human SCO2 is required for the synthesis of CO II and as a thiol-disulphide oxidoreductase for SCO1. Hum Mol Genet 18:2230–2240.
8. Leary SC, Cobine PA, Kaufmann BA, Guercin G, Mattman A, Palaty J, Lockitch G, Winge DR, Rustin P, Horvath R, Shoubridge EA (2007) The human cytochrome *c* oxidase assembly factors SCO1 and SCO2 have regulatory roles in the maintenance of cellular copper homeostasis. Cell Metab 5:9–20.
9. Leary SC (2010) Redox regulation of SCO protein function: controlling copper at a mitochondrial crossroad. Antioxid Redox Signal 13:1403–1416.
10. Williams JC, Sue C, Banting GS, Yang H, Glerum DM, Hendrickson WA, Schon EA (2005) Crystal structure of human SCO1: implications for redox signalling by a mitochondrial cytochrome c oxidase "assembly protein". J Biol Chem 280:15202–15211.
11. Glerum DM, Shtanko A, Tzagoloff A (1996) SCO1 and SCO2 act as high copy suppressors of a mitochondrial copper recruitment defect in *Saccharomyces cerevisiae*. J Biol Chem 271:20531–20535.
12. Banci L, Bertini I, Cavallaro G, Ciofi-Baffoni S (2011) Seeking the determinants of the elusive functions of Sco proteins. FEBS J 278:2244–2262.
13. Mansilla N, Racca S, Gras DE, Gonzalez DH, Welchen E (2018) The complexity of mitochondrial complex IV: an update of cytochrome c oxidase biogenesis in plants. Int J Mol Sci 19:662–696. https://doi.org/10.3390/ijms19030662.
14. Winge DR (2003) Let's Sco1, Oxidase! Let's Sco! Structure 11:1313–1314.
15. Carr HS, Winge DR (2003) Assembly of cytochrome c oxidase within the mitochondrion. Acc Chem Res 36: 309–316.
16. Robinson NJ, Winge DR (2010) Copper metallochaperones. Annu Rev Biochem 79:537–562.
17. Papadopoulou LC, Sue CM, Davidson MM, Tanji K, Nishino I, Sadlock JE, Krishna S, Walker W, Selby J, Glerum DM, Coster RV, Lyon G, Scalais E, Lebel R, Kaplan P, Shanske S, de Vivo DC, Bonilla E, Hirano M, DiMauro S, Schon EA (1999) Fatal infantile cardioencephalomyopathy with COX deficiency and mutations in SCO2, a COX assembly gene. Nat Genet 23:333–337.
18. Badrick AC, Hamilton AJ, Bernhardt PV, Jones CE, Kappler U, Jennings MP, McEwan AG (2007) PrrC, a Sco homologue from *Rhodobacter sphaeroides*, possesses thiol-disulfide oxidoreductase activity. FEBS Lett 581: 4663–4667.
19. Dash BP, Alles M, Bundschuh FA, Richter OH, Ludwig B (2015) Protein chaperones mediating copper insertion into the Cu_A site of the aa_3-type cytochrome c oxidase of *Paracoccus denitrificans*. Biochim Biophys Acta Bioenergetics 1847:202–211.
20. Rosenzweig AC (2001) Copper delivery by metallochaperone proteins. Acc Chem Res 34:119–128.
21. Gurumoorthy P, Ludwig B (2015) Deciphering protein-protein interactions during the biogenesis of cytochrome c oxidase from *Paracoccus denitrificans*. FEBS J 282:537–549.
22. Banci L, Bertini I, Cavallaro G, Rosato A (2007) The functions of Sco proteins from genome-based analysis. J Proteome Res 6:1568–1579.
23. Attallah CV, Welchen E, Martin AP, Spinelli SV, Bonnard G, Palatnik JF, Gonzalez DH (2011) Plants contain two SCO proteins that are differentially involved in cytochrome c oxidase function and copper and redox homeostasis. J Exp Bot 62:4281–4294.
24. Balatri E, Banci L, Bertini I, Cantini F, Ciofi-Baffoni S (2003) Solution structure of Sco1: a thioredoxin-like protein involved in cytochrome c oxidase assembly. Structure 11:1431–1443.
25. Chinenov YV (2000) Cytochrome c oxidase assembly factors with a thioredoxin fold are conserved among prokaryotes and eukaryotes. J Mol Med 78:239–242.
26. Nittis T, George GN, Winge DR (2001) Yeast Sco1, a protein essential for cytochrome c oxidase function, is a Cu(I)-binding protein. J Biol Chem 276:42520–42526.
27. Abajian C, Rosenzweig AC (2006) Crystal structure of yeast Sco1. J Biol Inorg Chem 11:459–466.
28. Siluvai GS, Mayfield M, Nilges MJ, Debeer George S, Blackburn NJ (2010) Anatomy of a red copper center: spectroscopic identification and reactivity of the copper centers of bacillus subtilis Sco and its Cys-to-ala variants. J Am Chem Soc 132:5215–5226.
29. Siluvai GS, Nakano M, Mayfield M, Blackburn NJ (2011) The essential role of the Cu(II) state of Sco in the maturation of the Cu_A center of cytochrome oxidase: Evidence from H135Met and H135SeM variants of the *Bacillus subtilis* Sco. J Biol Inorgan Chem 16:285–297.
30. Morgada MN, Abriata LA, Cefaro C, Gajda K, Banci L, Vila AJ (2015) Loop recognition and copper-mediated disulfide reduction underpin metal site assembly of Cu_A in human cytochrome oxidase. Proc Natl Acad Sci USA 112:11771–11776.
31. Maeda K, Hagglund P, Finnie C, Svensson B, Henriksen A (2006) Structural basis for target protein recognition by the protein disulfide reductase thioredoxin. Structure 14:1701–1710.
32. Banci L, Bertini I, Ciofi-Baffoni S, Gerothanassis IP, Leontari I, Martinelli M, Wang S (2007) A structural characterization of human SCO2. Structure 15: 1132–1140.
33. Andruzzi L, Nakano M, Nilges MJ, Blackburn NJ (2005) Spectroscopic studies of metal binding and metal selectivity in *Bacillus subtilis* BSco, a homolog of the yeast

mitochondrial protein Sco1p. J Am Chem Soc 127: 16548–16558.
34. Fraczkiewicz R, Braun W (1998) Exact and efficient analytical calculation of the accessible surface areas and their gradients for macromolecules. J Comput Chem 19: 319–333.
35. Zaballa M, Abriata LA, Donaire A, Vila AJ (2012) Flexibility of the metal-binding region in apo-cupredoxins. Proc Natl Acad Sci USA 109:9254–9259.
36. Williams PA, Blackburn NJ, Sanders D, Bellamy H, Stura EA, Fee JA, McRee DE (1999) The Cu_A domain of *Thermus thermophilus* ba_3-type cytochrome *c* oxidase at 1. 6 Å resolution. Nat Struct Biol 6:509–516.
37. Kallis GB, Holmgren A (1980) Differential reactivity of the functional sulfhydryl groups of cysteine-32 and cysteine-35 present in the reduced form of thioredoxin from *Escherichia coli*. J Biol Chem 255:10261–10265.
38. Armougom F, Moretti S, Poirot O, Audic S, Dumas P, Schaeli B, Keduas V, Notredame C (2006) Expresso: automatic incorporation of structural information in multiple sequence alignments using 3D-Coffee. Nucleic Acids Res 34:W604–W608.
39. Abicht HK, Scharer MA, Quade N, Ledermann R, Mohorko E, Capitani G, Hennecke H, Glockshuber R (2014) How periplasmic thioredoxin TlpA reduces bacterial copper chaperone ScoI and cytochrome oxidase subunit II (CoxB) prior to metallation. J Biol Chem 289: 32431–32444.
40. Siluvai GS, Nakano MM, Mayfield M, Nilges MJ, Blackburn NJ (2009) H135A controls the redox activity of the Sco copper center. Kinetic and spectroscopic studies of the His135Ala variant of *Bacillus subtilis* Sco. Biochemistry 48:12133–12144.
41. Carr HS, Georges GN, Winge DR (2002) Yeast Cox11, a protein essential for cytochrome c oxidase assembly, is a Cu(I)-binding protein. J Biol Chem 277:31237–31242.
42. Thompson AK, Gray J, Liu A, Hosler JP (2012) The roles of *Rhodobacter sphaeroides* copper chaperones PCu_AC and Sco (*PrrC*) in the assembly of the copper centers of the aa_3-type and the cbb_3-type cytochrome *c* oxidases. Biochim Biophys Acta Bioenerg 1817: 955–964.
43. Lohmeyer E, Schröder S, Pawlik G, Trasnea P, Peters A, Daldal F, Koch H (2012) The ScoI homologue SenC is a copper binding protein that interacts directly with the cbb_3-type cytochrome oxidase in *Rhodobacter capsulatus*. Biochim Biophys Acta Bioenerg 1817:2005–2015.
44. Hill BC, Andrews D (2012) Differential affinity of BsSCO for Cu(II) and Cu(I) suggests a redox role in copper transfer to the Cu A center of cytochrome c oxidase. Biochim Biophys Acta Bioenerg 1817:948–954.
45. Slutter CE, Sanders D, Wittung P, Malmstrom BG, Aasa R, Richards JH, Gray HB, Fee JA (1996) Water-soluble, recombinant Cu_A-domain of the cytochrome ba_3 subunit II from *Thermus thermophilus*. Biochemistry 35:3387–3395.
46. Eyer P, Worek F, Kiderlen D, Sinko G, Stuglin A, Simeon-Rudolf V, Reiner E (2003) Molar absorption coefficients for the reduced Ellman reagent: reassessment. Anal Biochem 312:224–227.
47. Pace CN, Vajdos F, Fee L, Grimsley G, Gray T (1995) How to measure and predict the molar absorption coefficient of a protein. Protein Sci 4:2411–2423.